

A Supervoid Imprinting the Cold Spot in the Cosmic Microwave Background

F. Finelli ^{1,2*}, J. García-Bellido ^{3†}, A. Kovács ^{4,5,‡}, F. Paci ^{6§}, I. Szapudi ^{7¶}

¹ INAF-IASF Bologna, Istituto di Astrofisica Spaziale e Fisica Cosmica di Bologna

Istituto Nazionale di Astrofisica, via Gobetti 101, I-40129 Bologna, Italy

² INFN, Sezione di Bologna, Via Irnerio 46, I-40126 Bologna, Italy

³ Instituto de Física Teórica IFT-UAM/CSIC, Universidad Autónoma de Madrid, Cantoblanco 28049 Madrid, Spain

⁴ Institute of Physics, Eötvös Loránd University, 1117 Pázmány Péter sétány 1/A Budapest, Hungary

⁵ MTA-ELTE EIRSA "Lendület" Astrophysics Research Group, 1117 Pázmány Péter sétány 1/A Budapest, Hungary

⁶ SISSA, Astrophysics Sector, Via Bonomea 265, 34136, Trieste, Italy

⁷ Institute for Astronomy, University of Hawaii, 2680 Woodlawn Drive, Honolulu, HI, 96822, USA

18 February 2022

ABSTRACT

The Cold Spot is one of the anomalies in the Cosmic Microwave Background, and could be of primordial origin, or caused by a foreground structure. The recently constructed WISE-2MASS all-sky infrared catalogue has a projected underdensity in the direction of the Cold Spot with an angular size 10's of degrees, and as deep as $\delta \simeq -0.12$ in the center. We show that a spherically symmetric Lemaitre-Tolman-Bondi (LTB) void model can simultaneously fit the underdensity in the WISE-2MASS catalogue and the Cold Spot as observed by both the Wilkinson Anisotropy Probe and Planck satellites. Such an LTB supervoid gives a perfect explanation, via a Rees-Sciama effect, of the Cold Spot anomaly, and is strongly preferred (using a Bayesian analysis) over the null hypothesis (statistical fluctuation) or a texture model. When the galaxy bias, measured from the large-scale angular power spectrum, is taken into account, a simultaneous three-parameter fit for the void model and the temperature profile gives $z_0 = 0.16 \pm 0.04$ for the mean redshift of the supervoid, $r_0 = 195 \pm 35 h^{-1} \text{Mpc}$ for its size, and $\bar{\delta} = -0.10 \pm 0.03$ for the top-hat-projected average depth of the void. These parameters are in excellent agreement with the results of Szapudi et al. (2014), who used additional photometric redshifts from Pan-STARRS1 for direct tomographic imaging of the void.

Key words: cosmic microwave background - large scale structure - inhomogeneous models

1 INTRODUCTION

The temperature anisotropies of the Cosmic Microwave Background (CMB) provide the earliest image of the primordial density fluctuations generated during inflation. They evolve into the present distribution of Dark Matter traced by galaxies, possibly in a biased fashion. The cosmological information encoded in the spatial distribution of galaxies is revealed by several present and future programs mapping the Universe in wide area surveys, such as Pan-STARRS (Kaiser et al. 2010), DES (The Dark Energy Survey Collaboration 2005), BigBOSS (Schlegel et al. 2011), LSST (LSST

Science Collaboration et al. 2009) and Euclid (Amendola et al. 2013).

While a homogeneous and flat Universe with dark matter and a cosmological constant - the Λ CDM model - is in agreement with most cosmological observations, it is challenged by several puzzling anomalies on large angular scales seen in the CMB patterns.

Among these anomalies, a cold area of approximately 5° radius in the direction ($b = -57^\circ, l = 209^\circ$), initially found in the Wilkinson Microwave Anisotropy Probe (WMAP) temperature map by Vielva et al. (2004), has been characterized in the *Planck* 2013 temperature maps with great accuracy (Ade et al. 2013). The occurrence of a decrement in the CMB temperature pattern with similar size in Gaussian simulations has been evaluated to be below 1% (Cruz et al. 2005). Thus a physical explanation for the Cold Spot (CS) is more plausible than a statistical fluke.

The CS in the CMB pattern could have been originated

* E-mail: finelli@iasfbo.inaf.it

† E-mail: juan.garciabellido@uam.es

‡ E-mail: andraspankas@gmail.com

§ E-mail: fpaci@sisa.it

¶ E-mail: szapudi@IfA.Hawaii.Edu

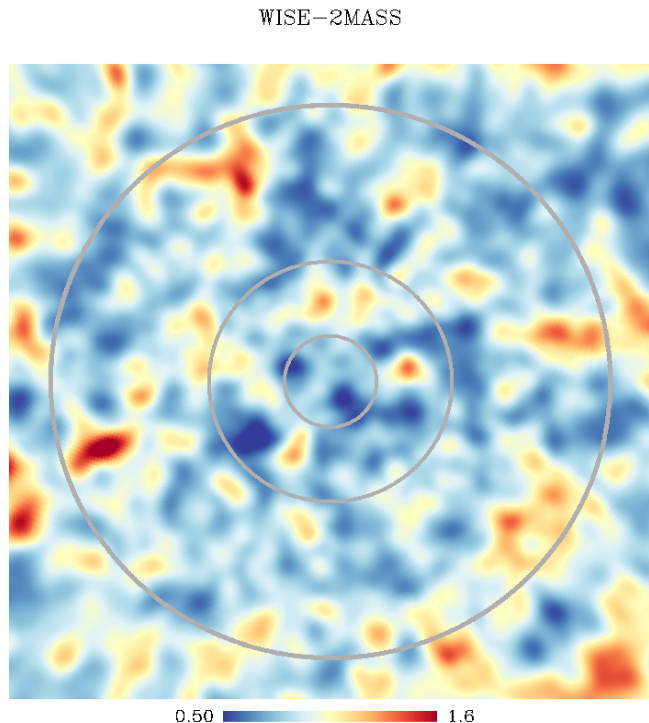


Figure 1. The WISE-2MASS map in the direction of the Cold Spot. Circles correspond to 5° , 13° and 28° radii.

by a primordial fluctuation on the last scattering surface or by an intervening phenomenon along the line of sight. Contamination from our galaxy or by the Sunyaev-Zeldovich effect from a cluster are quite unlikely (Cruz et al. 2006). If it were a primordial feature on the last scattering surface, the CS could be a signature of a non-perturbative effect during inflation (García-Bellido and Haugboelle 2008; Afshordi, Slosar and Wang 2011), or it might open a new exciting window onto the early Universe if caused by a cosmic texture generated during a phase transition at 10^{16} GeV (Cruz et al. 2007). Alternatively, the CS could be imprinted by an intervening supervoid along the line of sight (Inoue and Silk 2006, 2007; Inoue, Sakai and Tomita 2010; Inoue 2012; Masina and Notari 2009). While voids fill approximately 30 % of the Universe at $z < 1$ (Colberg et al. 2005) a quantitative explanation requires a supervoid with radius $\gtrsim 200 \text{ Mpc}^{-1}$, a quite rare structure in a ΛCDM cosmology.

The supervoid hypothesis can be tested in galaxy surveys, and several investigations have been already carried out. An underdensity in the direction of the CMB cold spot has been claimed in NVSS (Rudnick et al. 2007), but its statistical significance has been debated (Smith and Huterer 2010). Granett, Szapudi and Neyrinck (2010) imaged the cold spot region by the Canada-France-Hawaii Telescope (CFHT) ruling out the existence of a 100 Mpc supervoid with underdensity $\delta \simeq -0.3$ at $0.5 < z < 0.9$. Bremer et al. (2010) reached similar conclusions from a redshift survey using the VIMOS spectrograph on the VLT. In the relatively shallow 2MASS galaxy catalogue, Francis & Peacock (2010) found an under-density in the galaxy field in the Cold Spot

region. The structure they identified induces a $\Delta T = -7 \mu\text{K}$ depression in the CMB temperatures in the ΛCDM model, that is not a satisfactory explanation for the CS anomaly.

In this paper we jointly consider CMB and large scale structure data, and test the idea that an LTB supervoid could explain both observations. We use the recent galaxy catalogue WISE-2MASS (Kovács and Szapudi 2014) produced by joining the Wide-Field Infrared Survey Explorer (WISE, Wright et al. (2010)) with the 2-Micron All-Sky Survey (2MASS, Skrutskie et al. (2006)). See Kovács et al. (2013) for the previous generation of catalogue based on WISE alone. We consider WMAP-9yr and *Planck* as CMB data. To minimize astrophysical contamination we use foreground cleaned maps. For WMAP, we use the 9th year Internal Linear Combination (ILC) map at the HEALPIX (Gorski et al. 2005) resolution $N_{\text{side}} = 1024$ publicly provided at <http://lambda.gsfc.nasa.gov/>. For *Planck* data different CMB foreground cleaned maps are provided Ade et al. (2013), and we choose the Spectral Matching Independent Component Analysis (SMICA) (Cardoso et al. 2008) map at the HEALPIX (Gorski et al. 2005) resolution $N_{\text{side}} = 2048$, publicly provided at <http://pla.esac.esa.int/pla/aio/planckProducts.html>.

2 METHODS

Kovács and Szapudi (2014) combined photometric information of the WISE and 2MASS infrared all-sky surveys to produce a clean galaxy sample for large-scale structure research. They apply Support Vector Machines (SVM) to classify objects using the multicolor WISE-2MASS database. They calibrate their star-galaxy separator algorithm using Sloan Digital Sky Survey (SDSS, Abazajian et al. 2009) classification, and use the Galaxy and Mass Assembly (GAMA, Driver et al. 2011) spectroscopic survey for determining the redshift distribution of the WISE-2MASS galaxy sample.

Furthermore, Kovács and Szapudi (2014) pointed out that $W1_{\text{WISE}} - J_{2\text{MASS}} \leq -1.7$ with a flux limit of $W1_{\text{WISE}} \leq 15.2$ mag is a simple and effective star-galaxy separator, capable of producing results comparable to the multi-dimensional SVM classification. As a further refinement, another flux limit of $J_{2\text{MASS}} \leq 16.5$ mag is applied to have a fairly uniform all-sky dataset that is deeper than 2MASS and cleaner than WISE. The final catalogue has an estimated $\sim 2\%$ stellar contamination among 2.4 million galaxies with $z_{\text{med}} \approx 0.14$.

We construct a mask to exclude potentially contaminated regions near the Galactic plane using the dust emission map of Schlegel et al. (1998). We mask out all pixels with $E(B - V) \geq 0.1$, and regions at galactic latitudes $|b| < 20^\circ$, leaving $21,200 \text{ deg}^2$ for our purposes.

Fig. 1 shows a $40^\circ \times 40^\circ$ size patch of the WISE-2MASS galaxy catalogue centered on the CS at a resolution of approximately $30'$, i.e. HEALPIX (Gorski et al. 2005) of $N_{\text{side}} = 128$. The corresponding profile of the underdensity as a function of the angular distance from the center is shown in the upper panel of Fig. 3.

At the center of the CS, there is an approximately 16% underdensity in galaxy counts, extending to a radius over 20° . We followed Kovács et al. (2013); Szapudi et al. (2014), and estimated the bias of the galaxy catalog using *SpICE*

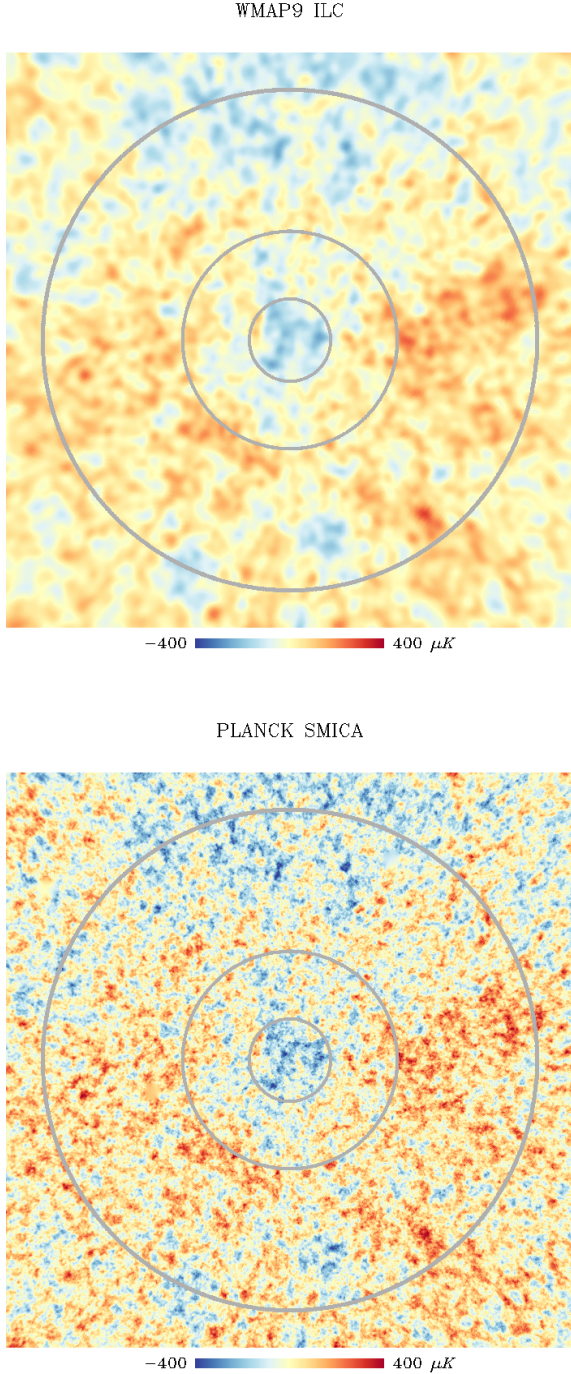


Figure 2. The WMAP-9yr (top) and Planck SMICA (bottom) in the direction of the Cold Spot. Circles correspond to 5° , 13° and 28° radii.

(Szapudi et al. 2001) and `python CosmoPy`¹ package, finding $b = 1.41 \pm 0.07$. The depression in galaxy counts, therefore, corresponds to a $\delta_{2D} \simeq -0.12$ underdensity in matter, assuming the linear bias relation $\delta_{2D} = \delta_{2D,g}/b$.

The image in the WISE-2MASS galaxy catalogue is

compared to the same angular patch of the WMAP-9yr Internal Linear Combination (ILC) map (Bennett et al. 2013) and of the *Planck* SMICA map (Ade et al. 2013). An average $50 \mu\text{K}$ temperature decrement of approximately 10° in size is clearly visible, corresponding to the CMB Cold Spot. The purpose of this letter is to show that a general relativistic void model for the underdensity in WISE-2MASS could explain the CMB cold spot.

3 THE LTB MODEL

We model the underdensity in the WISE-2MASS with a LTB model, (García-Bellido and Haugboelle 2008), characterized by a spatial curvature profile $k(r) = k_0 r^2 \exp(-r^2/r_0^2)$, which can be written as a linear metric perturbation in a ΛCDM model,

$$\Phi(\tilde{r}) = \Phi_0 e^{-\frac{\tilde{r}^2}{\tilde{r}_0^2}}, \quad (1)$$

with the LTB radius r related to the comoving FRW radius through $\tilde{r} = \sqrt{3/4\pi} H_0 r$. This scalar potential gives rise to a 3D density profile for the void

$$\delta(\tilde{r}) = -\delta_0 \left(1 - \frac{2\tilde{r}^2}{3\tilde{r}_0^2}\right) e^{-\frac{\tilde{r}^2}{\tilde{r}_0^2}}, \quad (2)$$

characterized by two parameters, the comoving width \tilde{r}_0 and the depth δ_0 . In order to compare with WISE-2MASS we project the 3D density (2) onto the transverse plane, using the WISE window function $\phi(y)$, with the center of the void at comoving distance y_0 , and $\tilde{r}^2(y, \theta) = y^2 + y_0^2 - 2yy_0 \cos \theta$,

$$\delta_{2D}(\theta) = \int_0^\infty \delta(\tilde{r}(y, \theta)) y^2 \phi(y) dy. \quad (3)$$

From the metric perturbation (1), we can also compute the linear Integrated Sachs-Wolfe (Sachs and Wolfe 1967) and the non-linear Rees-Sciama (Rees and Sciama 1968) effect on the CMB temperature anisotropies. For a large compensated void with a profile of Eq. 2, the linear ISW effect dominated by the non-linear Rees-Sciama effect,

$$\delta T(\theta) = -A \left(1 - \frac{28}{13} \frac{\theta^2}{\tilde{\theta}_0^2}\right) e^{-\frac{\theta^2}{\tilde{\theta}_0^2}}, \quad (4)$$

where $\tilde{\theta}_0 = \sqrt{3/4\pi} \theta_0$, and we used a small angle approximation, $\tan \theta \simeq \theta$. While the ISW effect is proportional to the time derivative of the potential, therefore typically smoother than the density distribution, the RS effect depends on higher derivatives, thus more compact than the void. This fact is reflected by the $\sqrt{3/4\pi} \simeq 0.48$ scaling factor between the scale of the void, and the scale of the corresponding cold spot on the CMB. The magnitude of the decrement depends on the parameters of the void,

$$A = 148.8 \mu\text{K} \left(\frac{r_0}{155.3 h^{-1} \text{Mpc}}\right)^3 \left(\frac{\delta_0}{0.2}\right)^2, \quad (5)$$

and $\theta_0 = (180^\circ/\pi)(r_0/d_A(z_0))$, with $d_A(z)$ the angular diameter distance in a flat ΛCDM model ($\Omega_M = 0.3, h = 0.7$), and z_0 the redshift of the center of the void, at comoving distance $y_0 = y(z_0)$. Qualitatively, a large LTB void can explain the CMB cold spot of about half the size. Moreover, compared to the linear ISW, the same decrement can be explained by a shallower void than is allowed by ΛCDM

¹ <http://www.ifa.hawaii.edu/cosmopy/>

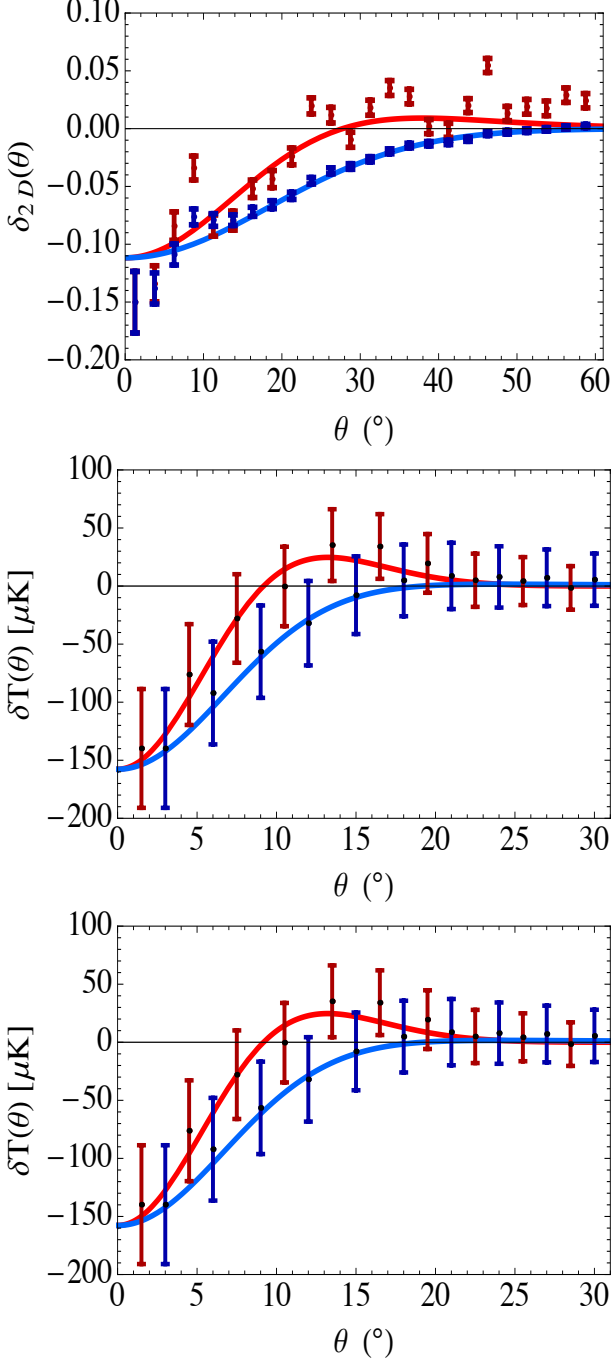


Figure 3. The density profile from WISE-2MASS catalogue compared with the theoretical model for the underdensity (3) (top panel). The temperature profile from WMAP-9yr ILC map (middle panel) and from *Planck* SMICA map (bottom panel) compared with the predicted signal (4). The red (blue) lines are the theoretical profiles for rings (disks) and in dark red (blue) are the measurements.

cosmology. Note that the LTB model is only used as a general relativistic model for the void dynamics and its effect on the CMB, while the background cosmology is assumed to be standard Λ CDM.

4 RESULTS

We construct a χ^2 corresponding to a simultaneous fit for the projected LTB void in the galaxy map, and the corresponding RS effect on the CMB. As primary parameters, we chose (δ_0, r_0, z_0) , giving the following:

$$\chi_{\text{tot}}^2(\delta_0, r_0, z_0) = \chi_{\text{LSS}}^2 + \chi_{\text{CMB}}^2, \quad (6)$$

$$\chi_{\text{LSS}}^2 = \sum_i \frac{(\delta_{2D}(\theta_i) - \delta_i^{\text{LSS}})^2}{\sigma_i^2}, \quad (7)$$

$$\chi_{\text{CMB}}^2 = \sum_{ij} \left(\delta T(\theta_i) - \delta T_i^{\text{CMB}} \right) C_{ij}^{-1} \left(\delta T(\theta_j) - \delta T_j^{\text{CMB}} \right) \quad (8)$$

The first term corresponds to the χ^2 of the projected LTB void profile (3) with respect to the observed WISE-2MASS galaxy distribution, using uncorrelated Poisson errors, σ_i . The second term is the χ^2 of the CMB profile compared with the LTB prediction (4) of the same void seen in the galaxy map. While Poisson fluctuations due to the discrete nature of galaxies are uncorrelated, the covariance matrix of rings in the CMB is highly correlated. Here the actual CMB fluctuations are considered as noise with respect to the RS effect we want to measure. The covariance matrix was determined from 10,000 Gaussian CMB realizations. Simultaneous minimization yields the best fit parameters, which we quote here with marginalized 1σ errors,

$$\delta_0 = 0.25 \pm 0.10 \ (1\sigma), \quad (9)$$

$$r_0(\text{Mpc}/h) = 195 \pm 35 \ (1\sigma), \quad (10)$$

$$z_0 = 0.155 \pm 0.037 \ (1\sigma). \quad (11)$$

The LTB model parameter δ_0 is the 3D Dark Matter density decrement, giving a 12% projected underdensity, i.e. $\delta_{2D}(\theta=0) = -0.12$, at the center of the void. The angular sizes $\theta_0 = 28.8^\circ \pm 5.2^\circ$, and $\tilde{\theta}_0 = 14.1^\circ \pm 2.5^\circ$ are derived parameters, representing the angular scales of the profile on the galaxy map and the CMB, respectively. Note that the radius of the LTB profile $\tilde{\theta}_0 = 14.1^\circ \pm 2.5^\circ$ on the CMB matches the outer hot ring around the cold spot discussed in Zhang and Huterer (2010).

For later comparison, we calculate the averaged underdensity within the best fit radius $r_0 = 195 h^{-1} \text{Mpc}$. The 3D top-hat-averaged density from the LTB profile, see Eq. (2), is $\bar{\delta} = 3/r_0^3 \int_0^{r_0} r^2 dr \delta(r) = -\delta_0/e$. This finally gives the average void depth $\bar{\delta} = -0.10 \pm 0.03$.

Note that our fit uses ring profiles only, but for illustration purposes we include in Fig. 3 the corresponding cumulative disk profiles, cautioning that the corresponding error-bars are correlated.

5 BAYESIAN MODEL COMPARISON

In order to correctly interpret the above results and weight the significance of the LTB void model, we consider as null hypothesis the case of the CS being a statistical fluctuation, and furthermore consider as a second hypothesis the phenomenological texture profile proposed by Cruz et al. (2008), which is characterized by a power-law $\delta T(\theta) = -A(1 + 4\theta^2/\theta_T^2)^{-1/2}$ matched to a Gaussian tail at angles larger than $\sqrt{3}\theta_T/2$. Since we don't have a density profile for

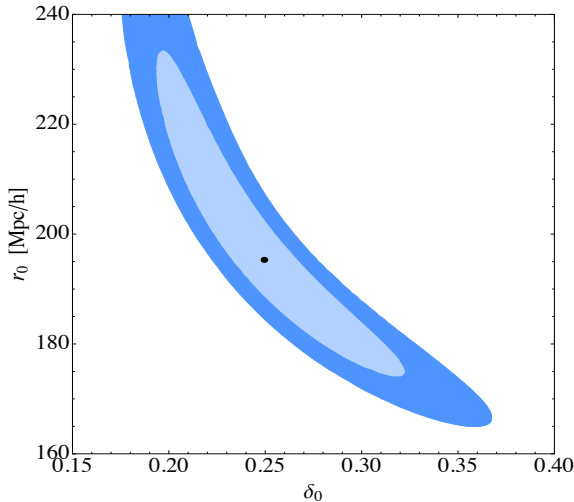


Figure 4. The 1 and 2σ contours of the size and depth parameters of the LTB void (2), after marginalization over the redshift of the center of the void with the WISE-2MASS window function.

the texture, we only compare the minimum χ^2_{CMB} for these three cases, using the *Planck* data:²

$$\chi^2_{\text{LTB}} = 7.06, \quad \chi^2_{\text{null}} = 27.35, \quad \chi^2_{\text{texture}} = 9.53. \quad (12)$$

We used 10 bins for the CMB profile, and fitted 3 parameters in the LTB void model, and thus we have $\nu = n - 3 = 7$ d.o.f. The minimum χ^2 of the LTB model is thus a very good fit, since the expectation is $\chi^2_{\text{min}} = \nu \pm \sqrt{2\nu} = 7 \pm 3.7$. The LTB and texture models are strongly preferred over the null hypothesis, and the LTB model is also preferred ($\Delta\chi^2 \simeq 2.5$) over the texture model, based on the χ^2 values alone.³

Next we calculate the Bayes factors for all three hypotheses, to gain more insight on the interpretation of the results. The evidence has been calculated integrating the full CMB likelihood over the priors. We chose non-informative uniform priors for both LTB, $\delta_0 \in (-0.3, 0)$, $r_0 \in (100, 300) h^{-1} \text{Mpc}$, and $z_0 \in (0, 0.3)$, and for the texture parameters, $A \in (-400, 0) \mu K$ and $\theta_T \in (0, 30^\circ)$,

$$\begin{aligned} \ln E_{\text{LTB}} &= -9.54, \\ \ln E_{\text{null}} &= -13.68, \\ \ln E_{\text{texture}} &= -15.47. \end{aligned} \quad (13)$$

Thus considering the Bayesian evidence, the LTB void is strongly favored, according to Jeffreys' scale, over both the null hypothesis and the phenomenological texture model.

Future data from CMB lensing (Das and Spergel 2008) and from 21-cm observations (Kovetz and Kamionkowski 2013) may help to further discriminate between the texture and the void hypotheses.

² WMAP-9yr data gives virtually identical results

³ Note that a physically motivated texture profile (Vilenkin & Shellard 1994), without matching to a Gaussian tail at large angles, would give $\chi^2_{\text{text}} \simeq 50$, i.e. significantly higher than the null hypothesis.

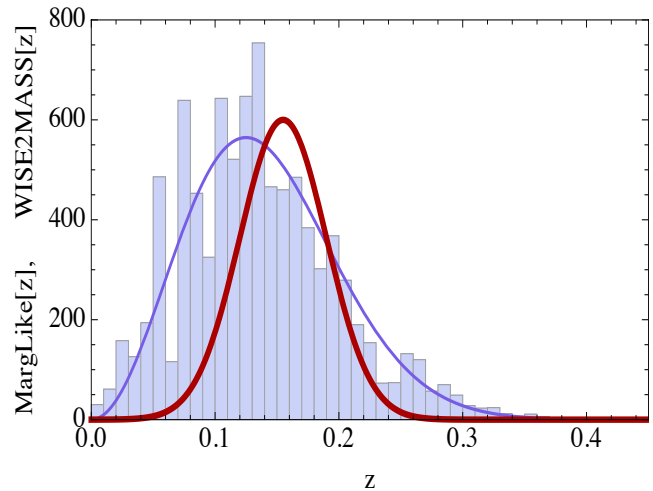


Figure 5. The marginalized redshift likelihood of the LTB void (in red), compared with the redshift distribution/histogram from WISE-2MASS (in blue).

6 CONCLUSIONS

In this Letter, we have shown for the first time that a large underdensity in the WISE-2MASS catalogue of Kovács and Szapudi (2014) could be imprinting the observed Cold Spot in the CMB. In particular, we show that both the void profile and the CMB profile can be simultaneously fit assuming an LTB profile embedded in an FRW universe located at redshift $z = 0.155 \pm 0.037$ with radius $r_0 = 195 \pm 35 h^{-1} \text{Mpc}$, and top-hat-averaged depth $\delta = -0.10 \pm 0.03$. Such an LTB supervoid gives a perfect explanation, via a Rees-Sciama effect, of the Cold Spot anomaly, and is strongly preferred (using a Bayesian analysis) over the null hypothesis (statistical fluctuation) or a texture model.

A related project Szapudi et al. (2014) used the same WISE-2MASS data set supplemented with PS1 photometric redshifts and the data by Granett, Szapudi and Neyrinck (2010) for a direct tomographic imaging of the CS region. They found a supervoid at $z = 0.22 \pm 0.01$ with radius $r_0 = 192 \pm 15 h^{-1} \text{Mpc}$ and depth of $\delta = -0.13 \pm 0.03$. These parameters are in excellent agreement with the findings of the present work, with the redshift slightly closer, but only by 1.75σ . Thus it is safe to conclude that the same supervoid was found with fundamentally different methods, and substantial difference between the two data sets: we do not have access to PS1 and Granett, Szapudi and Neyrinck (2010), while Szapudi et al. (2014) did not use any CMB data. Based on both of these works we conclude that the most plausible explanation of the CS is that it is due to a rare foreground supervoid structure that has been now identified in several data sets. Once photometric redshift will become available in the region, a precision LTB fit can be performed to refine these results further.

This Letter has provided a quantitative explanation of the CMB CS as a dominant RS effect due to a supervoid, here detected in the WISE-2MASS catalogue and described by an LTB profile. On scales larger than 25 degrees there is *only one* more underdensity in the WISE-2MASS catalogue, whose projected angular size is similar to the one in the direction of the CMB CS and is visible in the 2MASS

maps at lower redshifts (Francis & Peacock 2010). A thorough study of the connection between the most prominent underdensities of the WISE-2MASS all-sky survey catalog and the CMB temperature maps of Planck will be reported elsewhere.

ACKNOWLEDGEMENTS

FF and JGB wish to thank the bilateral agreement INFN-CICYT and in particular the director of the Bologna INFN section Dr. G. Bruni for partially supporting this project. FF acknowledges the support by ASI through ASI/INAF Agreement I/072/09/0 for the *Planck* LFI Activity of Phase E2 and by MIUR through PRIN 2009 grant no. 2009XZ54H2. JGB acknowledges financial support from the Madrid Regional Government (CAM) under the program HEPHA-COS S2009/ESP-1473-02, from the Spanish MICINN under grants AYA2009-13936-C06-06, FPA2012-39684-C03-02 and Consolider-Ingenio 2010 PAU (CSD2007-00060), and from the MINECO Centro de Excelencia Severo Ochoa Programme, under grant SEV-2012-0249. In addition, AK acknowledges support from Campus Hungary fellowship program, and OTKA through grant no. 101666. IS acknowledges support from NASA grants NNX12AF83G and NNX10AD53G.

REFERENCES

- Abazajian K. N., Adelman-McCarthy J. K., Agüeros M. A., Allam S. S., Allende Prieto C., An D., Anderson K. S. J., Anderson S. F., Annis J., Bahcall N. A., et al. 2009, *Astrophys. J. Suppl.* **182**, 543
- LSST Science Collaboration Abell P. A., Allison J., Anderson S. F., Andrew J. R., Angel J. R. P., Armus L., Arnett D., Asztalos S. J., Axelrod T. S., et al. 2009, *ArXiv e-prints*
- Ade P. A. R. *et al.* [Planck Collaboration], 2013, “Planck 2013 results. I. Overview of products and scientific results,” *arXiv:1303.5062 [astro-ph.CO]*.
- Ade P. A. R. *et al.* [Planck Collaboration], 2013, *arXiv:1303.5072 [astro-ph.CO]*.
- Ade P. A. R. *et al.* [Planck Collaboration], 2013, *arXiv:1303.5083 and arXiv:1303.5079 [astro-ph.CO]*.
- Afshordi N., Slosar A. and Wang Y., 2011, *JCAP* **1101** 019
- Amendola L. *et al.* [Euclid Collaboration], 2013, *Living Reviews in Relativity* **16**, 6
- Bennett C. L. *et al.* [WMAP Collaboration], 2013, *Astrophys. J. Suppl.* **208** 20
- Bennett C. L. *et al.* [WMAP Collaboration], 2003, *Astrophys. J. Suppl.* **148** 1
- Bremer M. N., Silk J., Davies L. J. M. and Lehnert M. D., 2010, *Mon. Not. Roy. Astron. Soc. Letters* **404** 69
- Cardoso J.-F., Martin M., Delabrouille J., Betoule M. and Patanchon G., 2008, *IEEE Journal of Selected Topics in Signal Processing* **2**, 735.
- Colberg J. M., Sheth R. K., Diaferio A., Gao L. and Yoshida N., 2005, *Mon. Not. Roy. Astron. Soc.* **360** 216
- Cruz M., Martinez-Gonzalez E., Vielva P. and Cayon L., 2005, *Mon. Not. Roy. Astron. Soc.* **356** 29
- Cruz M., Tucci M., Martinez-Gonzalez E. and Vielva P., 2006, *Mon. Not. Roy. Astron. Soc.* **369** 57
- Cruz M., Turok N., Vielva P., Martinez-Gonzalez E., and Hobson M., 2008, *Mon. Not. Roy. Astron. Soc.* **390** (2008) 913
- Cruz M., Martinez-Gonzalez E., Vielva P., Diego J. M., Hobson M. and Turok N., 2008, *Mon. Not. Roy. Astron. Soc.* **390** (2008) 913
- The Dark Energy Survey Collaboration
<http://www.darkenergysurvey.org/>
- Das S. and Spergel D.N., *Phys. Rev. D* **79** (2009) 043007
- Driver S. P., Hill D. T., et al. 2011, *Mon. Not. Roy. Astron. Soc.* **413**, 971
- Francis C. L., Peacock J. A., 2010, *MNRAS* **406**, 2
- Francis C. L., Peacock J. A., 2010, *MNRAS* **406**, 14
- García-Bellido J. and Haugboelle T., 2008, *JCAP* **0804** 003
- Gorski K. M., Hivon E., Banday A. J., Wandelt B. D., Hansen F. K., Reinecke M. and Bartelman M., *Astrophys. J.* **622** (2005) 759
- Granett B. R., Szapudi I. and Neyrinck M. C., 2010, *Astrophys. J.* **714** 825
- Inoue K. T. and Silk J., 2006, *Astrophys. J.* **648** 23
- Inoue K. T. and Silk J., 2007, *Astrophys. J.* **664** 650
- Inoue K. T., Sakai N. and Tomita K., 2010, *Astrophys. J.* **724**, 12
- Inoue K. T., 2012, *Mon. Not. Roy. Astron. Soc.* **421** 2731
- Francis C. L., Peacock J. A., 2010, *MNRAS* **406**, 14
- Kaiser N., Burgett W., Chambers K., 2010, ‘Society of Photo-Optical Instrumentation Engineers (SPIE) Conference Series’, 773
- Kovács A., Szapudi I., Granett B. R. and Frei Z., 2013, *MNRAS Letters* **431**, L 28.
- Kovács A. and Szapudi I., 2014, *arXiv:1401.0156*, submitted to *MNRAS*
- E. D. Kovetz and M. Kamionkowski, *Phys. Rev. Lett.* **110** (2013) 17, 171301
- Masina I. and Notari A., *JCAP* **0902** (2009) 019
- Rees, M. J. & Sciama, D. W., *Nature* **217** (1968) 511
- Rudnick L., Brown S. and Williams L. R., 2007, *Astrophys. J.* **671**, 40.
- Sachs, R. K. & Wolfe, A. M., *Astrophys. J.* **147** (1967) 73
- Schlegel, D. J. and Finkbeiner, D. P. and Davis, M., 1998, *arXiv:9710327*.
- Schlegel D., Abdalla F., Abraham T., Ahn C., Allende Prieto C., Annis J., Aubourg E., Azzaro M., Zhai C., Zhang P., 2011, *arXiv:1106.1706*.
- Smith K. M. and Huterer D., 2010, *Mon. Not. Roy. Astron. Soc.* **403** 2.
- Skrutskie M. F. et al., 2006, *Astron. J* **131**, 1163
- Szapudi, I. and Prunet, S. and Pogosyan, D. and Szalay, A. S. and Bond, J. R., 2001, *arXiv:0010256*
- Szapudi, I. et al., 2014, submitted.
- Vielva P., Martinez-Gonzalez E., Barreiro R. B., Sanz J. L. and Cayon L., 2004, *Astrophys. J.* **609** 22
- Vielva P., 2010, *Adv. Astron.* **2010** 592094.
- Vilenkin A. and Shellard E.P.S., “Cosmic Strings and other Topological Defects”, Cambridge U.P. (1994).
- Wright E. L. et al., 2010, *Astron. J* **140**, 1868
- Zhang R. and Huterer D., 2010, *Astropart. Phys.* **33**, 69